Nomenclature

a	= constant in Eq. (8)	[m^2/s]
a_v	= external area of particles per unit bed volume	[m^2/m^3]
A	= cross-sectional area effective for diffusion	[m^2]
b	= constant in Eq. (8)	[$m^2 \cdot$kg-adsorbent/s$\cdot$kg]
c	= adsorbate concentration	[kg/m^3]
d_p	= particle diameter	[m]
D_{AB}	= molecular diffusivity	[m^2/s]
D_{iq}	= intraparticle effective diffusivity based on amount adsorbed	[m^2/s]
D_K	= Knudsen diffusivity	[m^2/s]
D_p	= pore diffusivity	[m^2/s]
D_s	= surface diffusivity	[m^2/s]
E_a	= activation energy of surface diffusion	[J/mol]
k_s	= solid-phase mass transfer coefficient	[$kg/m^2 \cdot s$]
k^2	= tortuosity factor	[—]
K	= Langmuir constant	[m^3/kg]
L	= thickness of the diaphragm	[m]
M	= molecular weight	[—]
N	= total mass flow rate of adsorbate	[kg/s]
N_s	= mass flow rate of adsorbate due to surface diffusion	[kg/s]
N_0	= Avogadro's number	[mol^{-1}]
q	= amount adsorbed	[kg/kg-adsorbent]
q_∞	= Langmuir constant	[kg/kg-adsorbent]
R	= gas constant	[J/mol·K]
s	= cross-sectional area of one molecule adsorbed	[m^2]
S	= BET surface area	[m^2/kg]
t	= time	[s]
T	= temperature	[K]
x	= diffusional distance in the diaphragm	[m]
γ	= bed bulk density	[kg/m^3]
ε_p	= porosity	[—]
θ	= coverage	[—]
λ	= latent heat of evaporation	[J/mol]
ρ_s	= particle density	[kg/m^3]

〈Superscripts and Subscripts〉

$-$	= mean value
eff.	= effective value
h	= higher-concentration side of the diffusion cell
l	= lower-concentration side of the diffusion cell

Literature Cited

1) Glueckauf, E.: *Trans. Faraday Soc.*, **51**, 1540 (1955).
2) Kawazoe, K. and Y. Fukuda: *Kagaku Kōgaku*, **29**, 374 (1965).
3) Kawazoe, K., I. Sugiyama and Y. Fukuda: *Kagaku Kōgaku*, **30**, 1007 (1966).
4) Suzuki, M. and T. Fujii: *AIChE J.*, **28**, 380 (1982).
5) Takeuchi, Y., E. Furuya and H. Ikeda: *J. Chem. Eng. Japan*, **17**, 304 (1984).

EFFECTS OF NATURAL CONVECTION AND FLUID MIXING ON MASS TRANSFER BETWEEN PARTICLES AND FLUID IN PACKED BEDS

KENJI KUBO

Department of Industrial Chemistry, Osaka Prefectural Technical College, Neyagawa 572

HARUO HIKITA

Department of Chemical Engineering, University of Osaka Prefecture, Sakai 591

Key Words: Mass Transfer, Dissolution, Packed Bed, Natural Convection, Forced Convection, Fluid Mixing

Mass transfer between solid particles and a liquid flowing very slowly in packed beds is an important factor in determining the controlling rates in many mass transfer operations, such as ion exchange, adsorption, chromatography and catalytic processes. At very low flow rates, mass transfer in packed beds may be affected by natural convection and by axial fluid mixing. However, very few studies have been reported in the literature on the effects of these factors on the mass transfer rate. In the present work these problems were studied.

Received June 18, 1984. Correspondence concerning this article should be addressed to K. Kubo.

1. Theory

Consider dissolution from the surface of solid spherical particles in a packed bed into a liquid flowing very slowly. When the axial fluid mixing in the packed beds is assumed to be described by the side-mixing model proposed in a previous paper,[5] mass balances over a differential length of the packed bed yield the following equations in dimensionless form:

$$(1-\beta)\frac{\partial C_1}{\partial \tau} = -\frac{\partial C_1}{\partial \xi} + M(C_2 - C_1) \qquad (1)$$

$$\beta\frac{\partial C_2}{\partial \tau}=M(C_1-C_2)+N_L(C_s-C_2) \tag{2}$$

where

$$M=L/uR_M \tag{3}$$

and

$$N_L=k_L a_t L/u \tag{4}$$

The boundary conditions for Eqs. (1) and (2) are

$$\xi=0\,; \qquad C_1=C^{in}=0 \tag{5}$$

$$\xi=1\,; \qquad C_1=C^{out} \tag{6}$$

Under steady-state conditions, solution of Eqs. (1) and (2) gives the value of C^{out}, the solute concentration at the outlet of the packed bed, and is expressed as

$$C^{out}=C_s[1-e^{-MN_L/(M+N_L)}] \tag{7}$$

When it is assumed that no fluid mixing exists in the packed bed, the outlet solute concentration C^{out} under steady-state conditions can be given by

$$C^{out}=C_s(1-e^{-\hat{N}_L}) \tag{8}$$

where

$$\hat{N}_L=\hat{k}_L a_t L/u \tag{9}$$

Equating Eq. (7) and Eq. (8), the relationship between $\hat{N}_L$ and N_L is obtained as

$$\frac{1}{\hat{N}_L}=\frac{1}{N_L}+\frac{1}{M} \tag{10}$$

from which the relationship between $\hat{k}_L$ and k_L is expressed as

$$\frac{1}{\hat{k}_L}=\frac{1}{k_L}+R_M a_t \tag{11}$$

Therefore, when the values of R_M and a_t are known, the values of the true mass transfer coefficient k_L can be determined from the values of the apparent mass transfer coefficient $\hat{k}_L$.

In the previous paper,[3] mass transfer between solid particles in a packed bed and a flowing fluid in the laminar flow region, where both forced and natural convection are important, was analyzed theoretically on the basis of the free-surface model proposed by Happel.[2] According to this model, the average Sherwood number is given by

$$Sh=\frac{k_L d_p}{D}=\frac{\gamma}{1-\gamma}\int_0^{\pi}\frac{\eta_b \sin\theta}{I_1(\eta_b)}d\theta \tag{12}$$

Here γ and η_b are dimensionless parameters defined by

$$\gamma=(1-\varepsilon)^{1/3} \tag{13}$$

and

$$\eta_b=\left(\frac{d_p^2}{16D}\right)^{1/3}\left(\frac{1-\gamma}{\gamma}\right)\frac{\sqrt{\alpha}\sin^{1/2}\theta}{\left(\int_0^{\theta}\sqrt{\alpha}\sin^{3/2}\theta d\theta\right)^{1/3}} \tag{14}$$

Further, α in Eq. (14) can be obtained from the following equation:

$$\frac{d_p^2\alpha}{D\sin\theta}=6\left(\frac{1-\gamma^5}{W}\right)Pe+0.161\left(\frac{1-\gamma}{\gamma}\right)Ra\frac{\eta_b^2 I_2(\eta_b)-6I_4(\eta_b)}{\eta_b^3 I_1(\eta_b)} \tag{15}$$

where

$$W=2-3\gamma+3\gamma^5-2\gamma^6 \tag{16}$$

$$Pe=ScRe=d_p u/D \tag{17}$$

$$Ra=d_p^3\beta_e g(C_s-C_0)/\nu D \tag{18}$$

Thus, Eq. (12) with Eqs. (13) to (18) gives the theoretical values of the average Sherwood number under conditions of combined forced and natural convection as a function of Pe, Ra and γ or ε. When Ra is zero, the situation corresponds to pure forced-convection mass transfer in packed beds and Eq. (12) with Eqs. (14) and (15) leads to

$$Sh=1.25\left(\frac{1-\gamma^5}{W}\right)^{1/3}Pe^{1/3} \tag{19}$$

This equation agrees with that derived by Pfeffer.[6]

2. Experimental Apparatus and Procedure

The apparatus and experimental procedure employed were similar to those used by Williamson *et al.*[7] The packed column was an 8.0-cm inside diameter, 85.5 cm-high meta-acrylic resin tube. The inlet flow of the liquid was downflow through a packed bed of benzoic acid cylinders sandwiched between two layers of inert ceramic cylinders identical with the active benzoic acid cylinders. The 1.5 to 3.0 cm layer of active cylinders was located 7.0 cm from the bottom of the column. The active cylinders were pressed from reagent-grade benzoic acid in a polished steel mould by applying a pressure of about 200 MPa. The cylinders were 1.29 cm in outside diameter and 1.29 cm in height.

The liquid used was pure distilled water at 25°C and its flow rate was determined by collecting and weighing the outlet liquid for a measured time. After the system reached steady state, the outlet liquid was sampled and analyzed for benzoic acid by titration with 10 mol/m^3 NaOH solution using phenolphthalein as indicator. The precision of analysis was about 0.1%. Thus the error in the concentration driving force was less than 1%.

The values of the apparent mass transfer coefficient $\hat{k}_L$ were calculated from the following equation:

$$\hat{k}_L = \left(\frac{Q}{a_t}\right) \ln \frac{C_s - C^{in}}{C_s - C^{out}} \qquad (20)$$

3. Results and Discussion

The present experimental results, shown as a relationship between apparent Sherwood number $\widehat{Sh}$ and Reynolds number Re, were compared with previous data[1,4,7,8] on the dissolution of benzoic acid particles into water flowing slowly under downflow conditions and also with the theoretical line representing Eq. (19) derived by Pfeffer[6] for pure forced convection. For a non-spherical particle, the diameter of a sphere having the same surface area was used as the value of d_p. At higher Reynolds numbers ($Re > 10$), agreement between the present and previous data was fairly good and the data points were in good agreement with the theoretical line representing Eq. (19). At lower Reynolds numbers ($Re < 10$), where the data points scattered considerably, the present data agreed well with the data of Dryden *et al.*,[1] but were somewhat higher than the other previous data. Further, the present data deviated upward from the theoretical line representing Eq. (19) with increasing Re. This deviation might be due to the effects of natural convection and axial fluid mixing in the packed bed.

In **Fig. 1** the present experimental results are shown as a logarithmic plot of the Sherwood number $\widehat{Sh}$ or Sh vs. the Peclet number Pe and compared with the theoretical lines. In the case of dissolution of benzoic acid particles into water flowing slowly under downflow conditions, the natural convection currents have the same direction as the forced convection flow and increase the dissolution rates of benzoic acid. The dashed line in Fig. 1 shows Eq. (19), which is valid for pure forced convection, while the solid line represents Eq. (12) with Eqs. (13) to (18), which was derived for combined forced and natural convection. The difference between the solid and dashed lines represents the effect of natural convection on the Sherwood number, and this effect becomes quite pronounced at lower values of Pe. At higher values of Pe above 10^4, the solid line practically agrees with the dashed line and the open circles representing the measured values of $\widehat{Sh}$ are in good agreement with these theoretical lines. At lower values of Pe below 10^4, the data points (open circles) lie relatively above the dashed line, but fall considerably below the solid line. The difference between the solid line and the data points may be attributed to the effect of axial fluid mixing in the packed bed. The solid circles in Fig. 1 represent Sh values based on the k_L values calculated from the $\hat{k}_L$ values by using Eq. (11) and the empirical correlation for the side-mixing resistance R_M presented in the previous paper.[5] As can be seen in the figure, the data

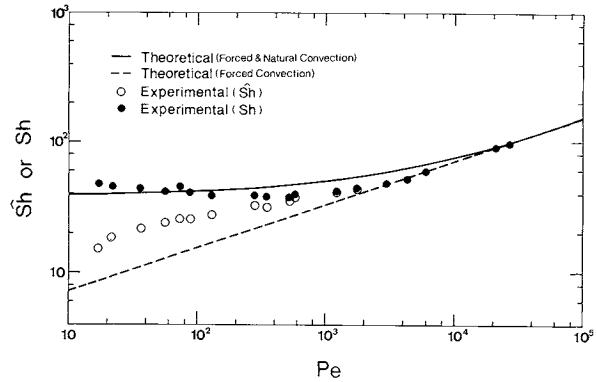

Fig. 1. Comparison of present experimental data with theoretical predictions.

points (solid circles) which were corrected for the effect of axial fluid mixing are in fairly good agreement with the solid line, although the experimental data are somewhat higher or lower than the theoretical line.

Nomenclature

a_t	=	total interfacial area of particles	[m^2]
C	=	solute concentration	[mol/m^3]
C_s	=	saturated solute concentration	[mol/m^3]
C_0	=	solute concentration in bulk fluid	[mol/m^3]
C_1	=	solute concentration in main-flow part	[mol/m^3]
C_2	=	solute concentration in side-flow part	[mol/m^3]
D	=	molecular diffusivity of solute	[m^2/s]
d_p	=	particle diameter	[m]
g	=	acceleration due to gravity	[m/s^2]
$I_n(\eta)$	=	function of η defined by	
		$\int_0^\eta \int_0^\eta \cdots \int_0^\eta \exp(-4\eta^3/9)(d\eta)^n$	[—]
k_L	=	average mass transfer coefficient	[m/s]
L	=	height of packed bed	[m]
M	=	side mixing factor, $L/R_M u$	[—]
N_L	=	number of transfer units, $k_L a_t L/u$	[—]
Pe	=	Peclet number, $d_p u/D$	[—]
Q	=	volumetric flow rate	[m^3/s]
R_M	=	side mixing resistance	[s]
Ra	=	Rayleigh number, $d_p^3 g \beta_e (C_s - C_0)/\nu D$	[—]
Re	=	Reynolds number, $d_p u/\nu$	[—]
Sc	=	Schmidt number, ν/D	[—]
Sh	=	average Sherwood number, $k_L d_p/D$	[—]
t	=	time	[s]
u	=	interstitial velocity, u_0/ε	[m/s]
u_0	=	superficial velocity in a packed bed	[m/s]
W	=	function of γ defined by Eq. (16)	[—]
x	=	axial distance	[m]
α	=	parameter defined by Eq. (15)	[—]
β	=	fraction of side-flow part	[—]
β_e	=	volumetric expansion coefficient of fluid	[—]
γ	=	parameter defined by Eq. (13)	[—]
ε	=	void fraction	[—]
η_b	=	parameter defined by Eq. (14)	[—]
ν	=	kinematic viscosity of fluid	[m^2/s]
τ	=	dimensionless time, ut/L	[—]
ξ	=	dimensionless height, x/L	[—]

⟨Superscripts⟩

^	=	apparent value
in	=	inlet value
out	=	outlet value

Literature Cited

1) Dryden, C. E., D. A. Strang and A. E. Withrow: *Chem. Eng. Progr.*, **49**, 191 (1953).
2) Happel, J.: *AIChE J.*, **4**, 197 (1958).
3) Hikita, H., K. Ishimi and K. Kubo: *Chem. Eng. Commun.*, **17**, 239 (1982).
4) Kataoka, T., H. Yoshida and K. Ueyama: *J. Chem. Eng. Japan*, **5**, 132 (1972).
5) Kubo, K., T. Aratani and A. Mishima: *Kagaku Kogaku Ronbunshu*, **7**, 304 (1981).
6) Pfeffer, R.: *Ind. Eng. Chem. Fundam.*, **3**, 380 (1964).
7) Williamson, J. E., K. E. Bazaire and C. J. Geankoplis: *Ind. Eng. Chem. Fundam.*, **2**, 126 (1963).
8) Wilson, E. J. and C. J. Geankoplis: *Ind. Eng. Chem. Fundam.*, **5**, 9 (1966).

MOISTURE PROFILE OF UNGLAZED ALUMINA-BASED CERAMIC ON CONVECTION DRYING

HIRONOBU IMAKOMA, MORIO OKAZAKI AND RYOZO TOEI

Department of Chemical Engineering, Kyoto University, Kyoto 606

Key Words: Convection Drying, Nonhygroscopic Material, Drying Model, Moisture Profile, Water Movement Model

Introduction

To express the water movement in an unsaturated porous body, we have proposed a modified Kozeny-Carman equation originating from the capillary action.[3,7] This equation was applied to the movement of condensed water in fine capillaries in an adsorptive porous body and it was found that the Kozeny constant varies inversely with the ratio of the amount of condensed water to the total moisture content: $K_c \propto X^*/X_l$.[8] This relation was confirmed by comparing the experimental drying data of an activated alumina rod with the calculated value.[9]

The object of this study is to confirm whether this simple relation can be applied to the movement of liquid water in fine capillaries in a non-hygroscopic porous body on drying, and to simulate the drying process using this water movement model and the drying model proposed by the authors.[7]

1. Experimental Results

The model material employed is an unglazed alumina-based ceramic. The experimental details are described in the previous study.[6] **Figure 1** indicates the cumulative curves of the pore volume and the surface area determined by the mercury penetration technique. The moisture content, X, can be calculated by the equation $X=\rho_l(V_t-V)$, using the cumulative pore-volume distribution, V, in this figure.

Figures 2 and **3** illustrate the experimental results. As may be seen from Fig. 3, the drying process was isothermal during all the period of drying except $t<2$ h in this experiment.

The critical moisture content was established during $5\,\text{h}<t_c<6\,\text{h}$ and the surface moisture content at this point X_c/X^* was 0.22 (see Fig. 2). The value of S_c determined from Fig. 1 is 1.09×10^2 m$^2\cdot$kg^{-1}. The value of X_c is equivalent to the maximum amount of unremovable pendular water.

2. Theory

It was found that liquid water in a non-hygroscopic capillary porous body classified into two groups[5]: funicular water capable of flowing in liquid state

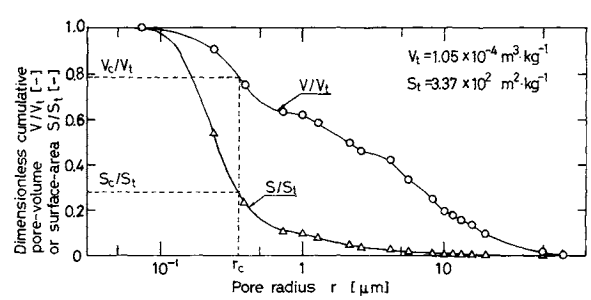

Fig. 1. Cumulative curves of pore volume and surface area. (Unglazed alumina-based ceramic.)

Received October 3, 1984. Correspondence concerning this article should be addressed to H. Imakoma.